Effect of gas properties on Diesel spray penetration and spreading angle for the ECN injectors

F. Payri, R. Payri*, F.J. Salvador, M. Bardi
CMT-Motores Térmicos, Universidad Politecnica de Valencia, Spain
fpayri@mot.upv.es, rpayri@mot.upv.es, fsalvado@mot.upv.es, mbardi@mot.upv.es

Abstract

The detailed knowledge of the Diesel spray formation is a key factor for the development of robust injection strategies able to reduce the pollutant emissions and keep or increase the combustion efficiency.

In this work, three similar single-hole injectors from engine Combustion Network (ECN) were compared measuring spray penetration and spreading angle under a wide range of test conditions. Several combinations of injection pressures (50 to 150 MPa) and ambient density (7.6 to 22.8 kg/m^3) have been tested in non-evaporative conditions in different gases: Nitrogen and Sulphur Hexafloride (SF_6); moreover, in Nitrogen atmosphere has been executed a temperature sweep from 300 to 550 K, while the same gas densities have been kept.

The single-hole nozzles from the ECN Working Group have been employed and n-dodecane has been used as fuel. The tests have been performed in two different test rigs: one designed for the recirculation of high density gases, like SF_6, at relatively low pressures (max 1 MPa); the other able to control both gas temperature and gas pressure over a wide range (300 – 1000 K and 0.1 – 15 MPa, respectively). Mie scattering imaging technique has been performed using a fast camera and a Matlab routine has been built for the image processing.

The experimental results pointed out some differences in spray penetration for the three injectors related mainly to start of injection transient and differences, spray orifice outlet diameter and spreading angle. A consistent effect of the type of the gas employed on spray penetration and spreading angle has been observed, while ambient temperature appears to have very small effect up 400K; above this temperature some reduction in penetration is appreciable due principally to limitation in the sensitivity of the technique when fuel evaporation is increasing. The non-complete momentum transfer between spray droplets and entrained gas as well as difference in sound speed probably are within the causes of the effect observed.

Introduction

Experimental investigation and modelling of Diesel spray are extremely challenging problems. The spray, especially in the neighbourhood of the nozzle, is very dense and the interaction between ambient gas and fuel takes place at microscopic scale (droplet diameter<30µm) and at high velocity (>100 m/s): this make the application of many conventional optical techniques (such as phase Doppler or PIV) very difficult. For this reason spray macroscopic characterization in cold conditions is still a widely employed technique to understand spray behaviour because it provides robust results with a relatively simple setup.

Engine Combustion Network [1] is an international collaboration aiming to link together experimental and modeling, addressing their research to reference test conditions. Five identical single orifice injectors have been donated by Bosch to ECN, and a number of measurement have been performed to compare results obtained in different test facilities [2] as well as to evaluate the techniques employed [3][4]. Most of these works have based their efforts assigning one of the injectors to each test facility and assuming an identical behavior as per manufacturer specification. On the other hand, internal nozzle geometry measurement (X-ray tomography, microscopic orifice imaging) [1] were pointing out some discrepancies between the *identical* injectors. At the same time most of the test were studying only the reference condition called *Spray A* (22.8 kg/m^3 ambient density, 150 MPa injection pressure, 900K ambient temperature and 15% O_2 concentration) being the first priority for ECN working group.

Isothermal macroscopic characterization of Diesel spray has demonstrated to be a robust measurement especially for spray penetration. On the other hand, spreading angle, which is an important indicator for spray-air mixing process, is very difficult to measure quantitatively and several studies linked its measurement with the optical setup employed or the processing method employed [5][6]. Spreading angle measurements still cannot be considered quantitative, however if any change in the optical setup is avoided, it enables qualitative comparisons.

This work focuses on the understanding of the different injectors' behavior beyond spray A conditions: three ECN injectors have been tested performing Mie scattering imaging in a wide range of ambient density and injection pressure, in isothermal conditions. The comparison between the injectors was performed using a high density gas (sulfur hexafluoride – SF_6) to simulate Diesel-like in cylinder density. Further tests have been performed to check the effect of spray composition and temperature on the measurement using Nitrogen and performing a temperature swipe from 300 to 550 K.

* Corresponding author: rpayri@mot.upv.es

Experimental Methods

Injection system

The injectors used in this study are three *identical* common rail solenoid actuated Bosch injectors equipped with a single axial hole with 90 µm nominal outlet diameter. The conical orifice (nominal *k-factor = 1.5)* and hydro-grinding were designed to avoid fuel cavitation in the orifice and to reach the discharge coefficient C_d = *0.86.* The injectors used are part of the five single-hole injectors employed by the Engine Combustion Network group (ECN). One of the steps of ECN analysis has been a deep characterization of the real injector internal geometry, and the results are available on the ECN web page [1]: the main characteristics of the injectors are listed in Table 1.

The injection system employed consists of commercial available components: a high pressure volumetric pump driven by an electric motor, a common rail with pressure regulator controlled by a PID system.

Injector #	Outlet diam. [µm]	Inlet diam [µm]	Nozzle length [µm]	K-factor [-]
Nominal	90	105	-	1.5
Uncertainty	1	2	5	0.1
210675	89.4	116	1030	2.7
210677	83.7	116	1026	3.2
210678	88.6	117	1044	2.8

Table 1: ECN nozzle internal geometry features. The data are obtained via X-ray tomography performed by *Caterpillar co.* [1]

Test chambers and Optical set up

Mie scattering spray imaging was performed in two different optical accessible test chambers. The first one, taking advantage of the SF_6 high density, was designed for relatively low pressures (max 0.6 MPa): hereafter this test rig will be referred as *test rig1* or *TR1*. The second test rig was used to analyse the effect of gas temperature on spray penetration from now on, this rig will be referred as *test rig 2* or *TR2*. Two Xe-arc light sources were used to illuminate the spray and a fast camera (Photron SX5) was employed to image the light scattered by fuel droplets. The tests rigs as well the details of the optical components employed in the tests are described below.

- *Test rig 1(*Figure 1*a):* the test rig was designed to study spray penetration in high density conditions at ambient temperature. High pressure needed to reach high density is normally an issue in the design: reduced chamber size as well as limited optical accessibility is an obvious consequence. *Test rig 1* was designed to obtain high density in the chamber employing Sulphur Hexafluoride, a gas with molecular weight six times higher than that of Nitrogen, that allows to reach high density limiting pressure employed. Despite maximum pressure allowed in the chamber by mechanical resistance is 0.8 MPa, densities up to 50 kg/m^3 can be achieved. A root compressor is used to recirculate the gas in a closed loop and to scavenge fuel droplet from the test chamber. *TR1* was used also to compare spray penetration and spreading angle in SF_6 and N_2 at relatively low ambient density (7.6 kg/m^3), the maximum reachable with Nitrogen. The facility is fully described in [2]. Figure 1*a* shows also the layout on injector light sources and camera: the two light sources are illuminating the two sides of the spray and the camera is collecting the light scattered perpendicularly.
- *Tests rig2* (figure 1b) this novel high temperature and high pressure vessel was designed to reach real Diesel engine in cylinder thermo-dynamic conditions within an optical accessible test chamber. A continuous high pressure gas flow is heated before entering the test chamber by a heating system. A PID system control the power supplied by the heaters and creates steady thermodynamic conditions in the test chamber.

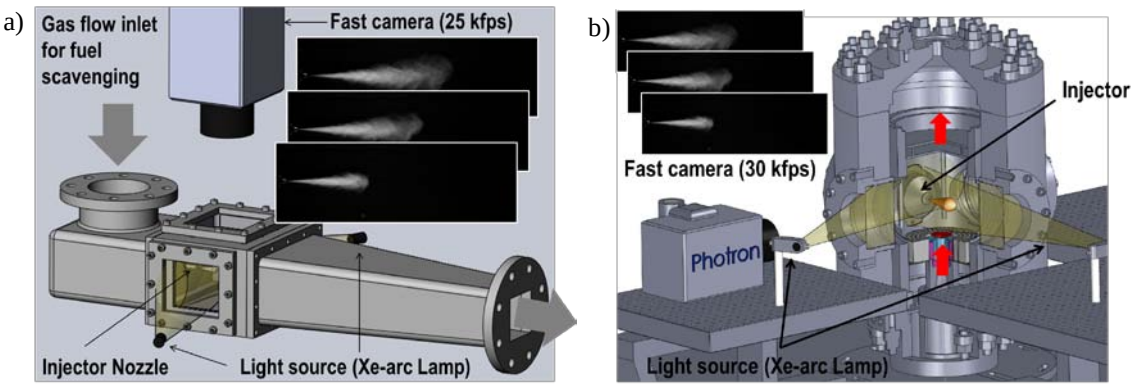

Figure 1. a) Sketch of the optical set up employed in *test rig 1* and b) in *test rig 2*

The wide optical access (3 windows of 128 mm diameter), the large test chamber (up to 110 mm free field) and limit test conditions (ambient temperature up to 1000 K and ambient pressure up to 15 MPa) make of this facilities one of the most advanced tools for Diesel spray study. The light sources have been arranged differently: one is pointing on spray from the same side of the camera while the second one is pointing the spray head on. In this way the illumination of the spray tip is optimized reducing sensitivity problems even when some evaporation is occurring. Despite Pickett et al. in [2] asses that head on illumination can introduce uncertainties on liquid length measurement, it has to be reminded that in this case the focus of the study is the effect of gas temperature on spray penetration. A complete description of the test rig is presented in [9].
The imaging system is detailed for the two cases in Table 2.

	Test rig 1	Test rig 2
Light source	double Xe-arc source	double Xe-arc source
Camera	Photron MX5	Photron MX5
Lens	Nikkor 50 mm f/1.8	Nikkor 50 mm f/1.8
Pixel/mm	7.44	11.7
Window size	20 x 95 mm	20 x 65 mm
Frame rate	30 kfps	25 kfps
Shutter time	15 µs	15 µs

Table 2: Details of imaging system employed in the two cases

Image Processing Method

Image segmentation is the first step for image processing: in the literature several approaches for image segmentation can be found [5]. In this study, thanks to the relatively flat background and the not-saturated images, a simple fixed threshold method has been employed: after the arithmetical subtraction of the background a threshold corresponding to 3% of the maximum digital level observed in the core of the spray is chosen for image binarization. This approach is widely used in Mie scattering imaging because it scales the sensitivity to the intensity of the illumination [9][10]. However, light orientation and camera non linearity at low counts number, have some effect on segmentation sensitivity: as shown in [5][11] spray penetration in non-evaporative conditions is a robust measurement because of the steep decrease at the spray tip in scattered intensity; its results are easily comparable in different setups. On the other hand, along radial profile droplet number density is decreasing smoothly [12][13] and Mie signal is very low at boundaries: in this case, segmentation method as well as optical setup becomes fundamental for the spreading angle measurement [12]. For this reason, in this study, spreading angle will be measured, but these results will be employed only for qualitative comparison between tests performed in the same test rig, when neither illuminating light intensity nor orientation are changed.

After image binarization, spray contour is processed to obtain the spray penetration and spreading angle computed as described by Naber and Siebers in [8].

Summarizing the method, the calculation requires an iterative process, since the definition used for each depends on the other. The penetration is defined as the distance along the spray axis S to a location where 1/2 of the pixels are on an arc of θ/2 are considered spray Figure 2.The spray angle, θ, is defined building the isosceles triangle with height S/2 and area A (Figure 2) and using the equation reported below.

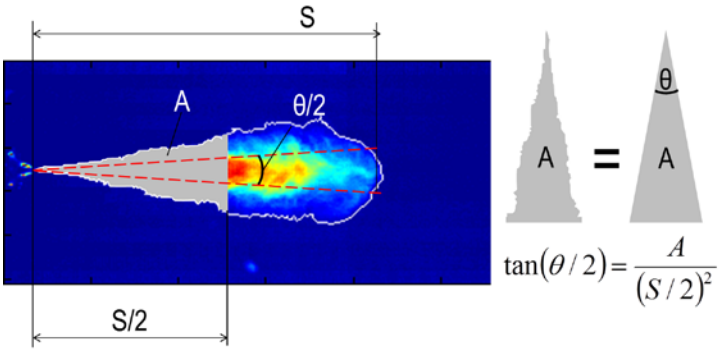

Figure 2. Sketch showing spray penetration (S) and spreading angle (θ) definition.

With the aim of laying a qualitative comparison between test conditions an average spreading angle θ_{av} was calculated. As discussed before, the algorithm used to measure spreading angle uses spray penetration to compute the area A. In order to lay a reliable comparison and take better into account the spray shape of cases with different penetration rate, the data used for the average θ_{av}, were selected with a penetration based criterion: the angle obtained for each test conditions is calculated averaging only the angles obtained when the penetration was included between 35 and 75 mm.

Test matrix

The spray penetration of three ECN injectors and the effect that gas composition and gas temperature have on it, has been investigated under a wide range of test conditions. The conditions tested and the test rig employed are detailed in Table 3.

Case 1		
Test rig	TR1	
Tamb [K]	300 K	
Nozzle #	675 - 677 - 678	
Gas	SF6	
Amb. density [kg/m3]	7.6 - 15.2 - 22.8	
Case 2		
Test rig	TR1	TR2
Tamb [K]	300 K	
Nozzle #	677	
Gas	Nitrogen	
Amb. Density [kg/m3]	7.6	7.6 - 15.2 - 22.8
Case 3		
Test rig	TR2	
Tamb [K]	from 300 to 550	
Nozzle #	677	
Gas	Nitrogen	
Amb. density [kg/m3]	22.8	

Table 3: Test matrix

Results and Discussion

Spray penetration at different test conditions is plotted in Figure 3a and 3b. Although the three injectors are always grouped closely for each test condition, a consistent difference between the three nozzles has been pointed out: injector 678 generally penetrates faster than the others, while 677 is the slowest one and 675 normally is in between. Shorter penetration of 677 is expected since, as shown in Table 1, the orifice outlet diameter is significantly smaller. However the difference between the injector is not always consistent and sometime the general trends mentioned above are not respected.

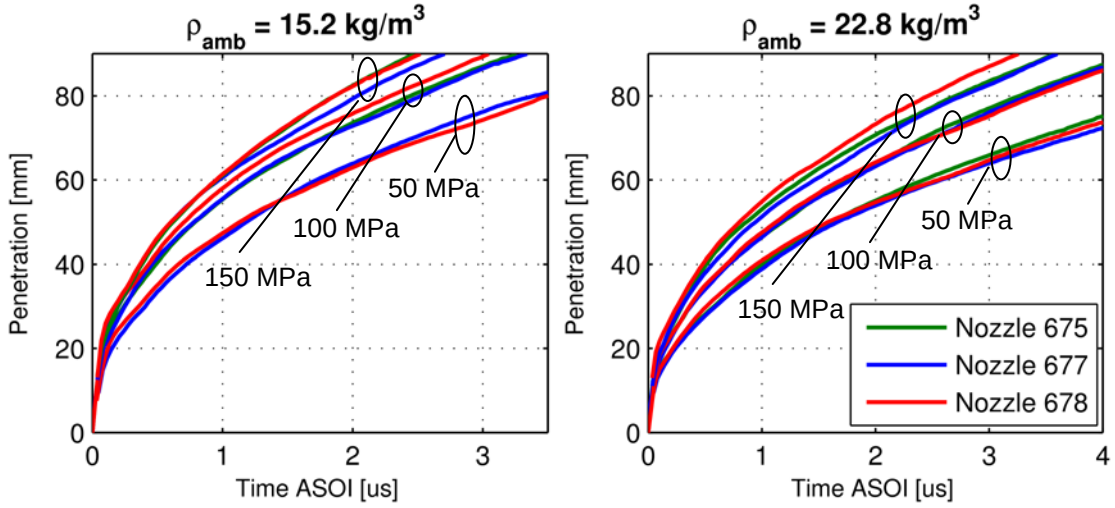

Figure 3: Spray penetration at different test conditions. The different injection pressures are grouped together. The data are related to tests in *test rig 1* with SF_6 atmosphere.

The value of the repetition to repetition standard deviation was checked to evaluate the consistency of the data. The standard deviation reported in the table presented in Figure 4 is obtained averaging the shot-to-shot standard deviation at each instant: in all the cases the standard deviation is lower than 2mm, and the value calculated for the whole dataset is 1.49 mm with similar results from the different injectors. This value suggests good test accuracy. However, in some cases the standard deviation is of the same order of magnitude of the differences observed in penetrations and for this reason more analysis is needed.

Another important parameter affecting the spray penetration is the spreading angle θ_{av}. The average spreading angle calculated allows to draw a global comparison including all the results obtained in the tests realized in

SF_6 atmosphere. As shown in Figure 4, there is a consistent and significant difference in spreading angle between the injectors: nozzle 677 has the largest spreading angle, while 678 the lowest. Another significant result showed by Figure 4 is that the influence of injection pressure for each injector is not the same: for example at 22.8 kg/m^3 ambient density, an increase in injection pressure causes a decrease in 678 spreading angle; on the other hand, the effect on injector 675 is the opposite. In this case the average standard deviation for the three injectors is 0.39º that is significantly lower than differences between injectors shown in Figure 4.

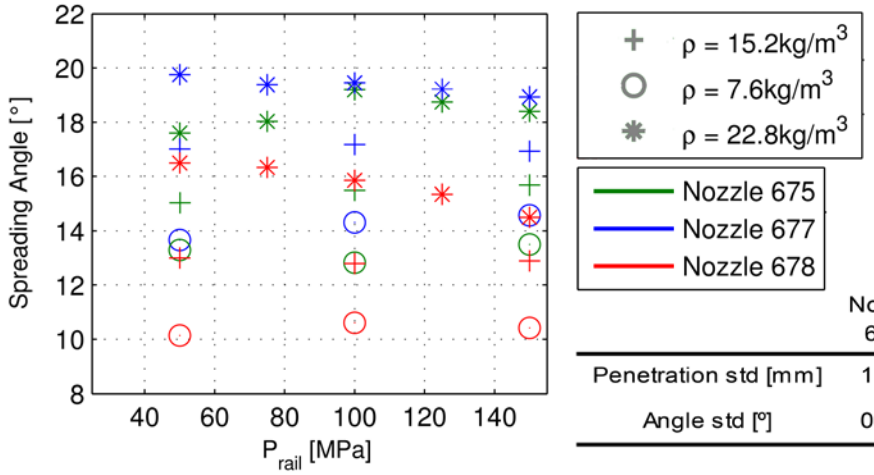

	Nozzle 675	Nozzle 677	Nozzle 678	Average
Penetration std [mm]	1.57	1.52	1.39	1.49
Angle std [º]	0.44	0.35	0.38	0.39

Figure 4: Average spreading angle θ_{av}, under different test conditions. The standard deviation value reported in the table is obtained averaging the shot-2-shot standard deviation calculated at each instant.

Before proceeding to a more quantitative analysis, the spray velocity has been analyzed calculating the time derivative of spray penetration, which practically is the spray tip velocity at a datum instant. The instantaneous spray velocity v_i is calculated with the time derivative $\Delta S/\Delta t$ where Δt and ΔS are respectively the variation in time and in penetration observed between two successive images. In order to reduce problem in shot-to-shot repeatability the velocity calculation is performed before the repetition average. Results for the three injectors are compared for two sample test conditions in Figure 5. To avoid that uncertainties in the opening transitory or SOI calculation have effect on the comparison between the injectors, on x-axis it is reported the spray penetration at corresponding velocity plotted in y-axis.

The plots show that the velocities calculated for the three sprays (and then in penetration) are related to fluctuation on the velocity probably linked with needle dynamics at the opening. In fact velocity of 678 is significantly higher only at the beginning. After the first transient, during which in some conditions tip velocity even increases, the velocities falls very close to each other's. This means that probably the part of the differences observed between the different injectors is not due to the flow in steady conditions but it is related to a dynamic response of the injector.

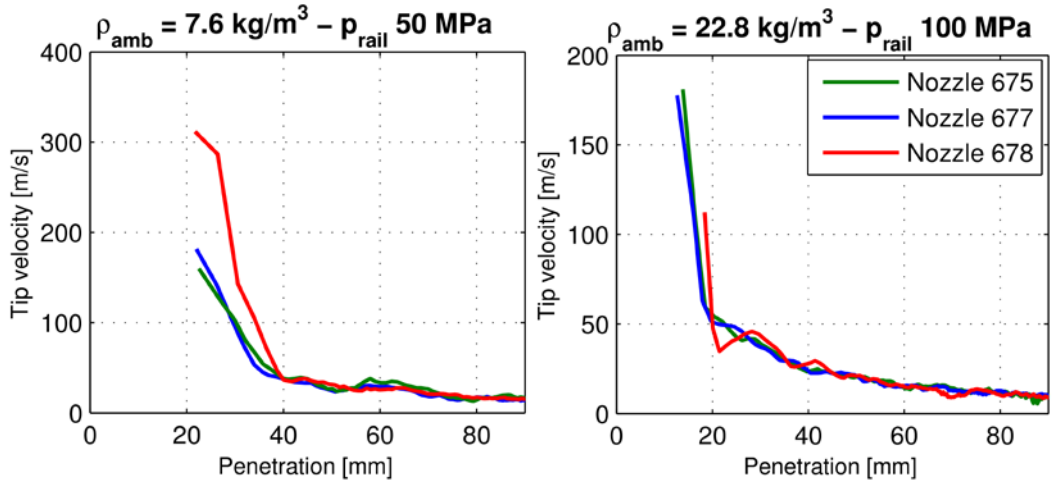

Figure 5: Tip velocity under different test conditions for the three ECN injectors.

A further test was performed to compare effect of spray penetration in SF6, and in Nitrogen at different pressures. The tests with Nitrogen at different temperature were performed in *test rig 2*. The main outcomes from the comparisons are described in the following paragraphs.

Faster penetration in SF_6 atmosphere: a significant difference in spray penetration between the Nitrogen cases and SF6 is observed: this fact is consistent in all the tests performed and was also observed by Payri et al. in [14]. In that case the cause of the increase in penetration was related to a variation in spreading angle but slight differences between the illumination employed for the comparison did not allow to be conclusive about the differences measured. In this work specific tests were performed in *test rig 1* with Nitrogen atmosphere at ρ_{amb} = 7.6 kg/m^3 that, due to mechanical resistance limitations, it is the highest density reachable with Nitrogen in *TR1*. In order to obtain a reliable comparison, nothing in the optical setup was changed from SF_6 tests. As in the previous comparison, tests in SF_6 showed faster penetration but this time a clear increase in spreading angle was proved. The variation observed in both penetration and spreading angle is difficult to explain and it is probably linked with changes at microscopic scale in the interaction between the ambient gas and fuel droplets and a less effective momentum transfer between fuel and ambient gases. Another fact, that has to be pointed out is a significant difference in sound speed *c:* the value of c_{SF6} (at 22.8 kg/m^3 and 300 K) is about 130 m/s; at the same temperature and density c_{N2} is about 356 m/s. Observing the plot of spray velocity in Figure 5 it is possible to see clearly that in SF_6 test, for a significant part of the injection, the spray is super-sonic while very few data above c_{N2} ware collected. Considering the discussion proposed by Roisman et al. in [15] there is a clear interaction between spray jet and pressure waves in the ambient at the beginning of the injection: without entering in the discussion, the authors want only to show a possible path to explain this deviation of the results.

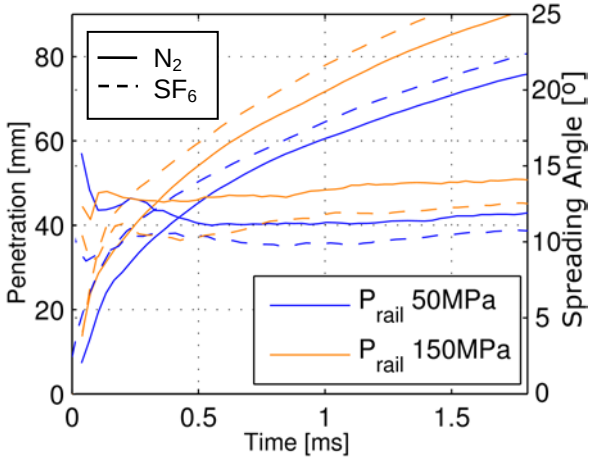

Figure 6: Penetration and spreading angle comparison in N_2 and SF_6. ρ_{amb} = 7.6 kg/m^3, TR 1

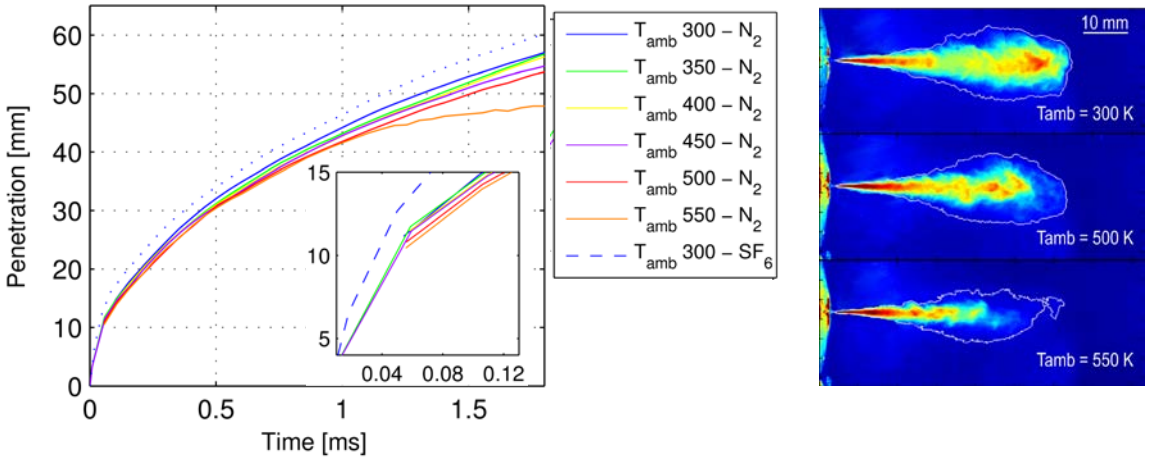

Figure 7: (a) Spray penetration measured at different ambient temperature and composition. The first penetration data are zoomed in order to compare different ambient temperatures. ρ_{amb} = 22.8 kg/m^3, p_{rail} = 150 MPa, nozzle 677. (b) Raw images acquired at different temperatures. TR1 for SF_6 tests and TR2 for tests in N_2.

Similar penetration at different Nitrogen temperatures: observing the results from the temperature swipe no significant differences are observed for $T_{amb} \leq 400$ K. For higher temperature a small decrease in spray penetration is observed especially when penetration is over 35-40 mm. At 550K the tip of the spray is missed com-

pletely as results of significant spray evaporation and lack of sensitivity of the technique. Figure 7b shows that, even if the penetration measured at 300 and 500K is similar, the distribution of the light scattered by the spray is significantly different as consequence of incipient fuel evaporation. For T_{amb} = 550K evaporation is too high and the algorithm is unable to detect all the spray jet. Even if the frame rate is not very high the increase of ambient temperature seems to have some effect shortening the first period of spray time-linear penetration (see below). This effect is coherent with what observed by Araneo in [16] and it is probably due to an improvement of momentum transfer between fuel and ambient gas linked to the evaporation taking place even if ambient temperature is lower than fuel boiling temperature.

In order to quantify the effect of each test conditions, the data obtained in the tests in SF_6 atmosphere were used for a statistical analysis. As described by Desantes et al. in [7], the penetration of the spray during the injection follows two behaviors: the first part characterized by a linear dependence with time, which at a certain bending distance switches in a second behavior when the spray is fully developed and the penetration is proportional to the square root of time. As observed above, during the first phase of injection, features related to injector's dynamics are observed and therefore the penetration is hardly predictable through a conventional model that considers sac pressure constant and equal to rail pressure. For this reason this analysis focuses on the fully developed spray excluding by the analysis all the points which penetration is lower than a value arbitrarily chosen for each ambient density (30 mm for 22.8 kg/m^3, 35 mm for 15.2 kg/m^3, and 40 mm for 7.6 kg/m^3). The equation employed for the regression is the one used by Payri et al. in [14] and it is presented below:

$$S = k \cdot \rho_{amb}^{a} \cdot \Delta p^{b} \cdot \tan\left(\theta_{av}/2\right)^{c} \cdot t^{d} \cdot \phi^{0.5} \qquad (1)$$

Where ρ_{amb} is ambient density, Δp is pressure difference between the rail and the pressure within the chamber, θ_{av} is the average angle measured at the instant corresponding test condition and *k*, *a*, *b*, *c*, and *d* are the parameters optimized in the regression. ϕ is the orifice outlet diameter obtained by orifice microscopy (Table 1).

The results of the regression are presented in Table 4. The high value of the R^2 obtained as well as the distribution of the points in Figure 8 underlines a good reliability of the correlation found.

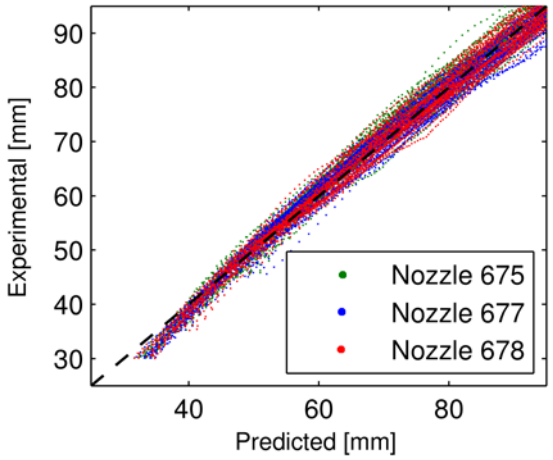

Figure 8: Spray penetration predictions vs experimental data

	k	a	b	c	d	R^2
From tests in SF_6	0.016	-0.33	0.24	-0.09	0.51	98.8
From tests in Air	0.010	-0.33	0.24	-0.09	0.54	98.6
From dim. analysis	-	-0.25	0.25	-0.5	0.5	-

Table 4: Results from regression of the data collected in SF_6 and air atmosphere to equation 1.

Summary and conclusions

Isothermal penetration of three "identical" ECN injector has been measured under a wide range of Diesel like test condition. The comparison of the three injectors has revealed the following features:

- Nozzle 677, according to orifice outlet measurement shows slower penetration. On the other hand nozzle 678 has the fastest penetration even if its diameter is slightly lower than that of 675.
- 678 spreading angle is substantially lower than the others and partially justify the higher penetration measured. Moreover, the relationship between injection pressure and spreading angle is not consistent between injectors as likely consequence of difference in internal flow.

- Observing the time derivative of the penetration it is pointed out that the biggest differences between injectors are observed in the very beginning of the injection and seems to be linked to injector needle dynamics.
- Penetration data obtained in SF_6 where compared to data obtained at the same test conditions (ambient temperature, ambient density and injection pressure) but in Nitrogen atmosphere: significant difference in spray penetration was observed. Specific tests shown that the spray angle in air is smaller as consequence of a different interaction between droplet and ambient gas. As a second path to explain the disagreement of the data, the dissimilarity in sound speed of the two gases has been pointed out.
- An ambient temperature swipe was performed in Nitrogen atmosphere to verify effect of temperature on penetration of non-evaporative spray: no significant difference is observed up to 400 K. while at 550 K consistent part of the spray is missed by the processing algorithm due to the incipient evaporation.
- A statistical analysis was performed and an equation was used for a regression to the experimental data. The results found gives good prediction of the data under all the conditions tested and shows good agreement with what found through dimensional analysis.

Acknowledgements

This work was sponsored by *"Ministerio de Ciencia e Innovación"* In the frame of the project "*Estudio teórico experimental sobre la influencia del tipo de combustible en los procesos de atomización y evaporación del chorro Diesel (PROFUEL)", Reference Nº TRA 2011-26293.*

The authors would like to thank also *Juan Pablo Viera* and *Jose Enrique del Rey* for their precious work in the laboratory during the tests.

Bibliography

[1] www.sandia.gov/ecn/

[2] Pickett, L., M., Genzale, C., Bruneaux, G., Malbec, L.-M., Hermant, L., Christiansen, C., Schramm, J., *Comparison of diesel spray combustion in different high-temperature, high pressure, facilities*, SAE international, SAE Paper 2010-01-2106, 2010

[3] Pickett, L., M.,, Genzale, C.,L., Manin, J., Malbec, L-M, Hermant, L., *Measurement Uncertainty of Liquid Penetration in Evaporating Diesel Sprays*, ILASS2011-111, 2011

[4] Nesbitt, J.E., Johnson, S.E., Pickett, L.M., Siebers, D.L., Lee, S-Y., Naber, J.D., 'Minor Species production from Lean Premixed Combustion and Their Impact on Autoignition of Diesel Surrogates,' Energy and Fuels 25 (3), pp. 926-936, 2011.

[5] Macian, V., Payri, R., Garcia, A., Bardi, M., Experimental Evaluation of the Best Approach for Diesel Spray Images Segmentation, Experimental Techniques, doi:10.1111/j.1747-1567.2011.00730.x, 2011

[6] Pastor J. V., Arrègle J., García J. M. and Zapata L. D, *Segmentation of diesel spray images with log-likelihood ratio test algorithm for non-Gaussian distribution*, Applied Optics, vol. 46 n. 6 (2007).

[7] Arrégle J., Pastor J. V. and Ruiz, S., *The influence of injection parameters on Diesel spray Characteristics*, SAE Paper 1999-01-0200, 1999

[8] Naber J.D., Siebers D.L., *Effects of gas density and vaporization on penetration and dispersion of diesel sprays*, SAE Paper 960034, (1996).

[9] Payri, R. and García-Oliver, J.M. and Bardi, M. and Manin, J., *Fuel temperature influence on Diesel sprays in inert and reacting conditions*, Applied thermal engineering, DOI: 10.1016/j.applthermaleng.2011.10.027, 2011

[10] Siebers, D.L., Scaling liquid-phase fuel penetration in Diesel sprays based on mixing-limited vaporization – SAE-1999-01-0528, 1999

[11] Payri F., Pastor J. V., Palomares A. and Julia J. E., *Optimal feature extraction for segmentation of Diesel spray images*, Applied Optics, vol. 40 (2001)

[12] Pickett, L., M., Manin, J., Genzale, C., L., Siebers, D., L., Musculus, M., Idicheria, C., *Relationship Between Diesel Fuel Spray Vapor Penetration/Dispersion and Local Fuel Mixture Fraction*, SAE International, 2011

[13] Payri, R. and Araneo, L. and Shakal, J. and Soare, V., *Phase doppler measurements: system set-up optimization for characterization of a diesel nozzle*, Journal of Mechanical Science and Technology, Vol 22 (8), pp. 1620-1632, 2008

[14] Payri, R., Salvador F. J., Gimeno, J., Soare V., *Determination of Diesel Spray Characteristics in Real Rngine In-Cylinder air Density and Presure Conditions*, Journal of Mechanical Science and Technology, pp 2040-2052, vol 19, 2005

[15] Roisman, IV and Araneo, L. and Tropea, C., *Effect of ambient pressure on penetration of a diesel spray*, International journal of multiphase flow, pp 904 - 920, vol. 33, 2007

[16] Araneo L., *Prediction of Diesel spray penetration with short injections in low density gas*, Thiesel Conference on Thermo- and Fluid Dynamic Processes in Diesel Engines, 2004